

Variational Monte-Carlo investigation of $SU(N)$ Heisenberg chains

Jérôme Dufour, Pierre Nataf, and Frédéric Mila

Institute of Theoretical Physics, École Polytechnique Fédérale de Lausanne (EPFL), CH-1015 Lausanne, Switzerland

(Dated: July 16, 2018)

Motivated by recent experimental progress in the context of ultra-cold multi-color fermionic atoms in optical lattices, we have investigated the properties of the $SU(N)$ Heisenberg chain with totally antisymmetric irreducible representations, the effective model of Mott phases with $m < N$ particles per site. These models have been studied for arbitrary N and m with non-abelian bosonization [I. Affleck, Nuclear Physics B 265, 409 (1986); 305, 582 (1988)], leading to predictions about the nature of the ground state (gapped or critical) in most but not all cases. Using exact diagonalization and variational Monte-Carlo based on Gutzwiller projected fermionic wave functions, we have been able to verify these predictions for a representative number of cases with $N \leq 10$ and $m \leq N/2$, and we have shown that the opening of a gap is associated to a spontaneous dimerization or trimerization depending on the value of m and N . We have also investigated the marginal cases where abelian bosonization did not lead to any prediction. In these cases, variational Monte-Carlo predicts that the ground state is critical with exponents consistent with conformal field theory.

I. INTRODUCTION

The possibility to load ultra cold fermionic atoms in optical lattices opens new perspectives in the investigation of lattice models of strongly correlated systems^{1,2}. When the optical lattice is deep enough, and when the fermionic atoms have an internal degree of freedom that can take N values (coming for instance from the nuclear spin in alkaline earths), the appropriate model takes the form of a generalized Hubbard model

$$\hat{H}_{\text{Hub}} = -t \sum_{\langle i,j \rangle} \sum_{\alpha=1}^N (\hat{a}_{i\alpha}^\dagger \hat{a}_{j\alpha} + \text{H.c.}) + \frac{U}{2} \sum_i \left(\sum_{\alpha} \hat{n}_{i\alpha} \right)^2$$

where $\hat{a}_{i\alpha}^\dagger$ and $\hat{a}_{i\alpha}$ are creation and annihilation fermionic operators, $\hat{n}_{i\alpha} = \hat{a}_{i\alpha}^\dagger \hat{a}_{i\alpha}$, t is the hopping integral between pairs of nearest neighbors $\langle i,j \rangle$, and U is the on-site repulsion.

When the average number of atoms per site m is an integer, and for large enough U/t , the system is expected to be in a Mott insulating phase³. Fluctuations induced by the hopping term in the manifold of states with m fermions per site start at second order in t/U , and the processes that appear at this order consist in exchanging particles between pairs of neighboring sites, leading to the effective Hamiltonian

$$\hat{H}_{\text{eff}} = \frac{2t^2}{U} \hat{H} \quad (1)$$

with

$$\hat{H} = \sum_{\langle i,j \rangle} \sum_{\alpha,\beta=1}^N \hat{a}_{i\alpha}^\dagger \hat{a}_{i\beta} \hat{a}_{j\beta}^\dagger \hat{a}_{j\alpha} \quad (2)$$

In the case of electrons with spin \uparrow or \downarrow , this Hamiltonian has $SU(2)$ symmetry, and it is equivalent to the Heisenberg model with coupling constant $4t^2/U$ thanks to the identity

$$\sum_{\alpha,\beta=\uparrow,\downarrow} \hat{a}_{i\alpha}^\dagger \hat{a}_{i\beta} \hat{a}_{j\beta}^\dagger \hat{a}_{j\alpha} = 2\vec{S}_i \cdot \vec{S}_j + \frac{1}{2} \hat{n}_i \hat{n}_j$$

and to the fact that $\hat{n}_i \hat{n}_j$ is a constant in the manifold of states with one particle per site.

More generally, when the number of degrees of freedom is equal to $N > 2$, Mott phases can be realized for all integer values of $m < N$. The effective model now has $SU(N)$ symmetry. This can be made explicit by introducing the generators

$$\hat{S}_{\alpha\beta} = \hat{a}_{\alpha}^\dagger \hat{a}_{\beta} - \frac{m}{N} \delta_{\alpha\beta}$$

which satisfy the $SU(N)$ algebra

$$[\hat{S}_{\alpha\beta}, \hat{S}_{\mu\nu}] = \delta_{\mu\beta} \hat{S}_{\alpha\nu} - \delta_{\alpha\nu} \hat{S}_{\mu\beta}$$

thanks to the identity

$$\sum_{\alpha,\beta=1}^N \hat{S}_{\alpha\beta}^i \hat{S}_{\beta\alpha}^j = \sum_{\alpha,\beta=1}^N \hat{a}_{i\alpha}^\dagger \hat{a}_{i\beta} \hat{a}_{j\beta}^\dagger \hat{a}_{j\alpha} - \frac{m^2}{N}$$

In the $SU(N)$ language, working with m fermions per site corresponds to working with the totally antisymmetric irreducible representation (irrep) that can be represented by a Young tableau with m boxes in one column. For any allowed m , there is a conjugate equivalent representation: a system with $m = k$ particles per site is equivalent to a system with $m = N - k$ particles per site.

The model Eq.2 captures the low-energy physics of multi-color ultra-cold atoms in optical lattices, systems for which remarkable progress has been recently achieved on the experimental side. For instance, the $SU(N)$ -symmetry has been observed in ultracold quantum gas of fermionic ^{128}Yb ⁴ or ^{87}Sr ⁵. Another example⁶ is the realization of one dimensional quantum wires of repulsive fermions with a tunable number of components.

The $SU(N)$ Heisenberg model with the fundamental representation at each site ($m = 1$), which corresponds to the Mott phase with one particle per site, has been investigated in considerable detail over the years. In one dimension, there is a Bethe ansatz solution for all values

of N^7 , and Quantum Monte Carlo simulations free of minus sign problem have given access to the temperature dependence of correlation functions^{8,9}. In two dimensions, a number of simple lattices have been investigated for a few values of N with a combination of semiclassical, variational and numerical approaches, leading to a number of interesting predictions at zero temperature^{10–25}.

In comparison, the case of higher antisymmetric irreps ($m > 1$) has been little investigated. In 2D, there is a mean-field prediction that chiral phases might appear for large m provided N/m is large enough^{26,27}, and some cases of self-conjugate irreps such as the 6-dimensional irrep of $SU(4)$ have been investigated with Quantum Monte Carlo simulations^{28–31} and variational Monte Carlo³². In 1D, apart from a few specific cases^{32–40}, including more general irreps than simply the totally antisymmetric ones, the most general results have been obtained by Affleck quite some time ago^{41,42}. Applying non-abelian bosonization to the weak coupling limit of the $SU(N)$ Hubbard model, he identified two types of operators that could open a gap: Umklapp terms if $N > 2$ and $N/m = 2$, and higher-order operators with scaling dimension $\chi = N(m-1)m^{-2}$ allowed by the $\mathbb{Z}_{N/m}$ symmetry if N/m is an integer strictly larger than 2. This allowed him to make predictions in four cases: i) N/m is not an integer: the system should be gapless because there is no relevant operator that could open a gap; ii) $N > 2$ and $N/m = 2$: the system should be gapped because Umklapp terms are always relevant; iii) N/m is an integer strictly larger than 2 and $\chi < 2$: the system should be gapped because there is a relevant operator allowed by symmetry. This case is only realized for $SU(6)$ with $m = 2$; iv) N/m is an integer strictly larger than 2 and $\chi > 2$: the system should be gapless because there is no relevant operator allowed by symmetry. The only case where the renormalization group argument based on the scaling dimension of the operator does not lead to any prediction is the marginal case $\chi = 2$, which is realized for two pairs of parameters: ($SU(8)$ $m = 2$) and ($SU(9)$ $m = 3$). These predictions are summarized in [TAB. I](#). Finally, in all gapless cases, the system is expected to be in the $SU(N)_{k=1}$ Wess-Zumino-Witten universality class^{41,43}, with algebraic correlations that decay at long distance with a critical exponent $\eta = 2 - 2/N$.

$N =$	3	4	5	6	7	8	9	10	$N/m \notin \mathbb{N}$	
$m = 1$									$m = 1$	} Gapless
$m = 2$									$\chi > 2$	
$m = 3$									$\chi = 2$	} ?
$m = 4$									$\chi < 2$	
$m = 5$									$N/m = 2$	} Gapped

TABLE I. Summary of the predictions of Refs. [41](#) and [42](#) for a representative range of $SU(N)$ with m particles per site. Note that models with $m = k$ and $m = N - k$ are equivalent up to a constant. Therefore the light gray shaded region can be deduced from the other cases and does not need to be studied.

To make progress on the general problem of the $SU(N)$

Heisenberg model with higher antisymmetric irreps, it would be very useful to have flexible yet reliable numerical methods that would allow to test these predictions in a systematic way. In particular, the methods should not be limited to 1D, or to cases such as self-conjugate irreps, for which there is a minus-sign free Quantum Monte Carlo algorithm. In this paper, we have decided to test the potential of Gutzwiller projected wave functions by a systematic investigation of the 1D case discussed by Affleck using variational Monte Carlo (VMC). There are two main reasons for this choice. First of all, these wave functions have been shown to be remarkably accurate in the case of the $SU(4)$ Heisenberg chain with the fundamental representation by Wang and Viswanath¹⁵, who have in particular shown that they lead to the exact critical exponent in that case. Besides, this approach can be easily generalized to higher dimensions, as already shown for the fundamental representation in a number of cases^{24,44}. Moreover, it has been used by Paramekanti and Marston³² for the self-conjugate representation in one and two dimensions.

In parallel, exact diagonalizations based on the extension of a recent formulation by two of the present authors⁴⁵ will be used whenever possible to benchmark the VMC approach on small clusters and, in some cases, to actually confirm the physics on the basis of a finite-size analysis.

As we shall see, the combination of these approaches leads to results that agree with Affleck's predictions whenever available, and to the identification of the symmetry breaking pattern in the gapped phases. In addition, it predicts that the marginal cases are gapless with algebraic correlations.

The paper is organized as follows. The next section describes the methods, with emphasis on the variational wave functions that will be used throughout. The third section is devoted to a comparison of the results obtained using the simplest wave functions (with no symmetry breaking) with those of the Bethe ansatz solution for the $m = 1$ case, with the conclusion that the agreement is truly remarkable. The fourth section deals with the cases where Umklapp processes are present ($N > 2$, $N/m = 2$), while the fifth one deals with the case where there is no Umklapp process but a relevant operator ($SU(6)$ $m = 2$). The marginal cases are dealt with in the sixth section, and the case where N/m is an integer without relevant nor Umklapp operators in the seventh section. Finally, the critical exponents are computed and compared to theoretical values for all gapless systems in the eighth section.

II. THE METHODS

A. Gutzwiller projected wave functions

The variational wave functions investigated in the present paper are obtained from fermionic wave functions

that have on average m particles per site by applying a Gutzwiller projector \hat{P}_G^m that removes all states with a number of particles per site different from m :

$$\hat{P}_G^m = \prod_{i=1}^n \prod_{p \neq m} \frac{\hat{n}_i - p}{m - p} \quad (3)$$

where n is the number of sites, and where the product over p runs over all values from 0 to N except $p = m$.

In the present paper, we will concentrate on simple fermionic wave-functions that, before projection, correspond to the ground state of trial Hamiltonians that contain only hopping terms. For $SU(2)$, the inclusion of pairing terms have been shown to lead to significant improvements⁴⁶, but the generalization to $SU(N)$ is not obvious because one cannot make an $SU(N)$ singlet with two sites as soon as $N > 2$. In addition, in the case of the fundamental representation where Bethe ansatz results are available for comparison, these simple wave functions turn out to lead to extremely precise results as soon as $N > 2$.

In practice, the construction of a Gutzwiller projected wave function starts with the creation of a trial Hamiltonian \hat{T} that acts on n sites and is written with fermionic operators $\hat{a}_{i\alpha}$ and $\hat{a}_{i\alpha}^\dagger$. When different colors are involved in \hat{T} , and as long as there is no term mixing different colors, the Hamiltonian can be rewritten as a direct sum: $\hat{T} = \bigoplus_{\alpha=1}^N \hat{T}_\alpha$. Then, for each color, there will be one corresponding unitary matrix U^α that diagonalizes \hat{T}_α . So the new fermionic operators are given by:

$$\hat{c}_{i\alpha} = \sum_{j=1}^n U_{ij}^{\alpha\dagger} \hat{a}_{j\alpha} \quad \hat{c}_{i\alpha}^\dagger = \sum_{j=1}^n U_{ji}^\alpha \hat{a}_{j\alpha}^\dagger,$$

and the trial Hamiltonian can be written in a diagonal basis:

$$\hat{T} = \bigoplus_{\alpha=1}^N \sum_{i=1}^n \omega_{i\alpha} \hat{c}_{i\alpha}^\dagger \hat{c}_{i\alpha}$$

with $\omega_{i\alpha} < \omega_{i+1\alpha}$.

In the Mott insulating phase, the system possesses nm/N particles of each color and exactly m particles per site. By filling the system with the nm/N lowest energy states of each color, the resulting fermionic wave function contains nm particles:

$$|\Psi\rangle = \bigotimes_{\alpha=1}^N \prod_{i=1}^{nm/N} \hat{c}_{i\alpha}^\dagger |0\rangle = \bigotimes_{\alpha=1}^N \prod_{i=1}^{mn/N} \sum_{j=1}^n U_{ji}^\alpha \hat{a}_{j\alpha}^\dagger |0\rangle \quad (4)$$

in terms of which the variational wave function is given by

$$|\Psi_G\rangle = \hat{P}_G^m |\Psi\rangle. \quad (5)$$

Since the Heisenberg model exchanges particles on neighboring sites, the simplest trial Hamiltonian that

allows the hopping of particles and its corresponding Gutzwiller projected wave function are:

$$\hat{T}_\alpha^{\text{Fermi}} = \sum_{i=1}^n \left(\hat{a}_{i\alpha}^\dagger \hat{a}_{i+1\alpha} + \text{H.c.} \right) \rightarrow |\Psi_G^{\text{Fermi}}\rangle.$$

In cases where a relevant or Umklapp operator is present, the ground state is expected to be a singlet separated from the first excited state by a gap, and to undergo a symmetry breaking that leads to a unit cell that can accommodate a singlet. In practice, this means unit cells with $d = N/m$ sites. To test for possible instabilities, we have thus used wave functions that are ground states of Hamiltonians that creates d -merization:

$$\hat{T}_\alpha^{t_i} = \sum_{i=1}^n \left(t_i \hat{a}_{i\alpha}^\dagger \hat{a}_{i+1\alpha} + \text{H.c.} \right) \rightarrow |\Psi_G^d(\delta)\rangle.$$

Assuming that the mirror symmetry is preserved, the wave functions $|\Psi_G^d(\delta)\rangle$ for dimerization ($d = 2$) and trimerization ($d = 3$) have only one allowed free parameter δ , and the hopping amplitudes in a unit cell are given by:

$$\begin{cases} t_i = 1 - \delta & \text{if } i = d \\ t_i = 1 & \text{otherwise.} \end{cases}$$

To test for a possible tetramerization for $SU(8)$ $m = 2$, since the unit cell contains four sites, one additional free parameter is allowed (still assuming that the mirror symmetry is preserved in the ground state). Therefore, we have used the wavefunction $|\Psi_G^4(\delta_1, \delta_2)\rangle$ with hopping amplitudes defined by:

$$\begin{cases} t_i = 1 - \delta_1 & \text{if } i = 2 \\ t_i = 1 - \delta_2 & \text{if } i = 4 \\ t_i = 1 & \text{otherwise.} \end{cases}$$

This method is always well defined for periodic boundary conditions when N/m is even. But when N/m is odd, the ground state is degenerate for periodic boundary conditions if the translation symmetry is not explicitly broken, and one has to use anti-periodic boundary conditions for $|\Psi_G^{\text{Fermi}}\rangle$, $|\Psi_G^d(0)\rangle$ ($d = 2, 3$) and $|\Psi_G^4(0, 0)\rangle$.

The hope is that if \hat{T} is wisely chosen, then $|\Psi_G\rangle$ captures correctly the physics of the ground state, i.e. with a good variational wave function, $E_G \equiv \langle \Psi_G | \hat{H} | \Psi_G \rangle \approx E_0$, the exact ground state energy. To check the pertinence of this statement, we have compared the energies and nearest-neighbor correlations with those computed with ED on small systems with open boundary conditions. In the table [TAB. II](#), one can see, for some systems, the comparison between ED and VMC results for the ground state energy. The nearest-neighbor correlations will be compared in the next sections. Considering the excellent agreement between the two methods for the cluster sizes available to ED, there are good reasons to hope that these Gutzwiller projected wave functions can quantitatively describe the properties of the ground state.

N	m	n	ED	VMC	error [%]
4	2	16	-1.6971	-1.6916	-0.33
4	2	18	-1.6925	-1.6866	-0.35
6	2	15	-2.7351	-2.7287	-0.23
6	3	12	-4.0295	-4.0261	-0.08
6	3	14	-4.0162	-4.0123	-0.10
8	2	12	-3.1609	-3.1587	-0.07
8	2	16	-3.1857	-3.1828	-0.09
9	3	9	-6.0960	-6.0810	-0.25
9	3	12	-6.1162	-6.0980	-0.30
10	2	15	-3.3992	-3.3919	-0.21

TABLE II. Comparison between the ED and VMC energies per site. The incertitudes on the VMC data are smaller than 10^{-4} . The relative error is always smaller than 0.35%.

B. Exact diagonalizations

On a given cluster, the total Hilbert space grows very fast with N , and the standard approach that only takes advantage of the conservation of the color number is limited to very small clusters for large N . Quite recently, two of the present authors have developed a simple method to work directly in a given irrep for the $SU(N)$ Heisenberg model with the fundamental representation at each site⁴⁵, allowing to reach cluster sizes typical of $SU(2)$ for any N . This method can be extended to the case of more complicated irreps at each site, in particular totally antisymmetric irreps, and the exact diagonalization results reported in this manuscript have been obtained along these lines.

C. Correlation function and structure factor

To characterize the ground state, it will prove useful to study the diagonal correlation defined by:

$$C(r) = \sum_{\alpha} \langle \hat{S}_{\alpha\alpha}^0 \hat{S}_{\alpha\alpha}^r \rangle = \sum_{\alpha} \langle \hat{a}_{0\alpha}^{\dagger} \hat{a}_{0\alpha} \hat{a}_{r\alpha}^{\dagger} \hat{a}_{r\alpha} \rangle - \frac{m^2}{N}. \quad (6)$$

The structure factor is then given by the Fourier transform of this function:

$$\tilde{C}(k) = \frac{1}{2\pi} \frac{N}{m(N-m)} \sum_r C(r) e^{ikr} \quad (7)$$

where the prefactor has been chosen such that:

$$\sum_k \tilde{C}(k) = \frac{n}{2\pi}.$$

III. $SU(N)$ WITH $m = 1$

In this section, we extend the $SU(4)$ results of Wang and Vishwanath¹⁵ to arbitrary N for $m = 1$ (fundamental representation), and we perform a systematic comparison with Bethe ansatz and Quantum Monte-Carlo

(QMC) results. Since these systems are known to be gapless, $|\Psi_G^{\text{Fermi}}\rangle$ is the only relevant wave function to study.

Let us start with the ground state energy. Using Bethe ansatz, Sutherland⁷ derived an exact formula for the ground state energy per site $e_0(N)$ of the Hamiltonian Eq.2 that can be written as a series in powers of $1/N$:

$$e_0(N) = -1 + 2 \sum_{k=2}^{\infty} \frac{(-1)^k \zeta(k)}{N^k} \quad (8)$$

where $\zeta(k) = \sum_{n=1}^{\infty} (1/n^k)$ is Riemann's zeta function. $e_0(N)$ is depicted in FIG. 1 as a continuous line. The dashed lines are approximations obtained by truncating the exact solution at order N^{-k} , $k \geq 2$. For comparison, the variational energies obtained in the thermodynamic limit after extrapolation from finite size systems are shown as dots in FIG. 1. The agreement with the exact solution is excellent for all values of N , and it improves when N increases (see table TAB. III). Quite remarkably, the variational estimate is better than the N^{-4} estimate even for $SU(3)$.

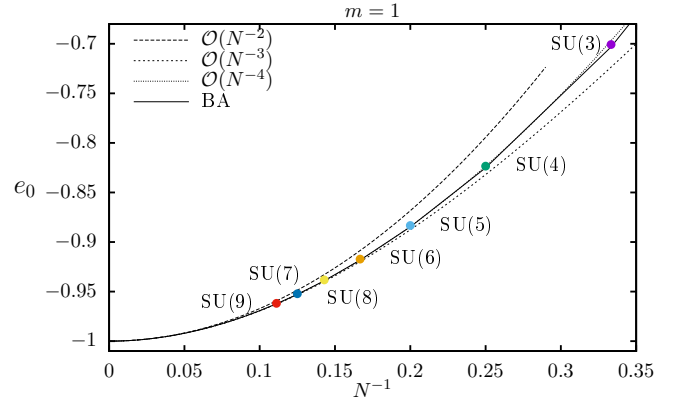


FIG. 1. Variational energy per site of $SU(N)$ chains with the fundamental irrep at each site (dots) compared to Bethe ansatz exact results (solid line) and polynomial approximations in $1/N$ (dashed lines).

N	BA	VMC	error [%]
3	-0.7032	-0.7007	-0.36
4	-0.8251	-0.8234	-0.21
5	-0.8847	-0.8833	-0.16
6	-0.9183	-0.9173	-0.11
7	-0.9391	-0.9383	-0.09
8	-0.9528	-0.9522	-0.06
9	-0.9624	-0.9620	-0.05

TABLE III. Comparison of the variational energies for $m = 1$ systems obtained for infinite chains with exact Bethe ansatz. The incertitudes on the VMC data are smaller than 10^{-4} .

We now turn to the diagonal correlations and its associated structure factor defined by Eq.6 and Eq.7. At very low temperature, QMC has been used by Frischmuth

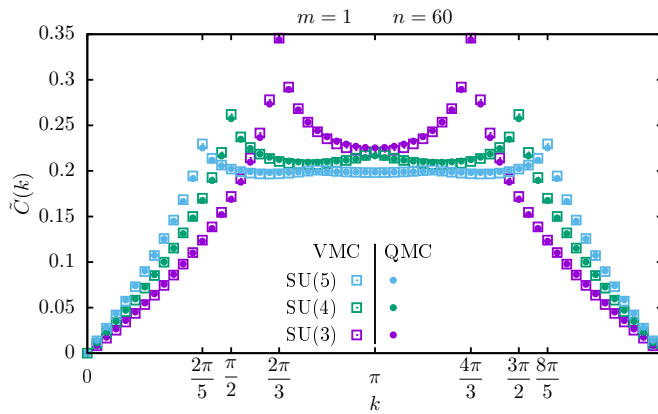


FIG. 2. Comparison of the structure factors calculated with VMC (empty squares) and QMC (filled circles) for various $SU(N)$ systems. In the VMC calculations, anti-periodic boundary conditions have been used for $SU(3)$ and $SU(5)$, and periodic ones for $SU(4)$.

*et al*⁸ for $SU(4)$ and by Messio and Mila⁹ for various values of N to compute this structure factor. The QMC data of Messio and Mila and the results obtained with VMC for $n = 60$ sites are shown in FIG. 2. Qualitatively, the agreement is perfect: VMC reproduces the singularities typical of algebraically decaying long-range correlations. But even quantitatively the agreement is truly remarkable, and, as for the ground state energy, it improves when N increases. Clearly, Gutzwiller projected wave functions capture the physics of the $m = 1$ case very well.

IV. $SU(N)$ WITH $m = N/2$

For these systems, there is a self-conjugate antisymmetric representation of $SU(N)$ at each site. The ground states of such systems, referred to as extended valence bound solids⁴⁷, are predicted to break the translational symmetry, to be two-fold degenerate and to exhibit dimerization since only two sites are needed to create a singlet, and the spectrum is expected to be gapped.

We have investigated two representative cases, ($SU(4)$ $m = 2$) and ($SU(6)$ $m = 3$), with ED up to 18 and 14 sites respectively, and the cases $N = 4$ to 10 with VMC. The main results are summarized in FIG. 3.

Let us start by discussing the ED results. Clusters with open boundary conditions have been used because they are technically simpler to handle with the method of Ref. 45, and because, in the case of spontaneous dimerization, they give directly access to one of the broken symmetry ground states if the number of sites is even. The gap as a function of the inverse size is plotted in the upper left panel of FIG. 3 for $SU(4)$ and $SU(6)$. In both cases, the results scale very smoothly, and a linear fit is consistent with a finite and large value of the gap in the thermodynamic limit. In the lower panels of FIG. 3, the bond energy is plotted as a function of the bond position

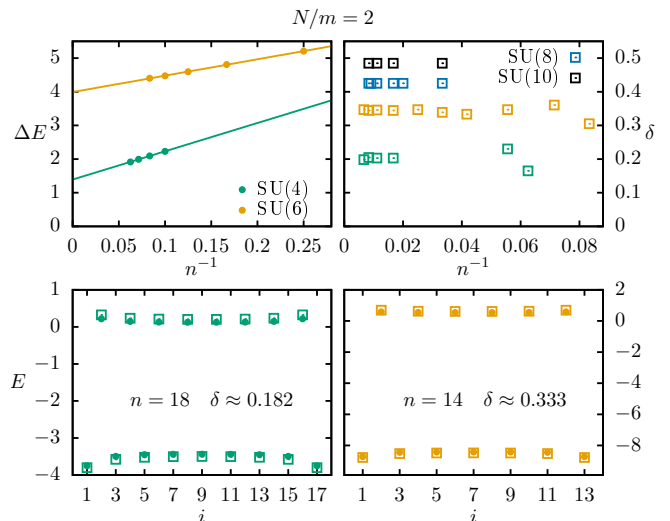


FIG. 3. ED and VMC results for various $SU(N)$ models with $m = N/2$. Upper left panel: size dependence of the energy gap for $SU(4)$ and $SU(6)$. Upper right panel: optimal variational parameter δ for periodic boundary conditions for $SU(4)$, $SU(6)$, $SU(8)$, and $SU(10)$. Lower panels: energy per bond for $SU(4)$ (left) and $SU(6)$ (right) calculated with ED (circles) and VMC (squares) for open boundary conditions. Note that the optimal variational parameters δ_{opt} are different in the upper right panel and in the lower panels because they correspond to different boundary conditions (periodic and open).

for the largest available clusters (18 sites for $SU(4)$, 14 sites for $SU(6)$) with solid symbols. A very strong alternation between a strongly negative value and an almost vanishing (slightly positive) value with very little dependence on the bond position clearly demonstrates that the systems are indeed spontaneously dimerized.

Let us now turn to the VMC results. Since the relevant instability is a spontaneous dimerization, it is expected that the dimerized $|\Psi_G^2(\delta)\rangle$ wave function allows one to reach lower energy than the $|\Psi_G^{\text{Fermi}}\rangle$ one. This is indeed true for all cases we have investigated (up to $N = 10$ and to $n \gtrsim 100$), and the optimal value of the dimerization parameter $\delta_{\text{opt}} > 0$ is nearly size independent and increases with N (see upper right panel of FIG. 3), in qualitative agreement with the gap increase between $SU(4)$ and $SU(6)$ observed in ED. To further benchmark the Gutzwiller projected wave functions for these cases, we have calculated the bond energy using the optimal value of δ (open symbols in the lower panel of FIG. 3) for the same clusters as those used for ED with open boundary conditions. The results are in very good quantitative agreement.

With the large sizes accessible with VMC, it is also interesting to calculate the diagonal structure factor defined in Eq. 7. All the structure factors peak at $k = \pi$, but, unlike in the case of the fundamental representation, there is no singularity but a smooth maximum (see FIG. 4). This shows that the antiferromagnetic corre-

lations revealed by the peak at $k = \pi$ are only short ranged, and that the correlations decay exponentially at long distance, in agreement with the presence of a gap, and with the spontaneous dimerization.

To summarize, ED and VMC results clearly support Affleck's predictions that the $N/m = 2$ systems are gapped and point to a very strong spontaneous dimerization in agreement with previous results by Paramakanti and Marston³².

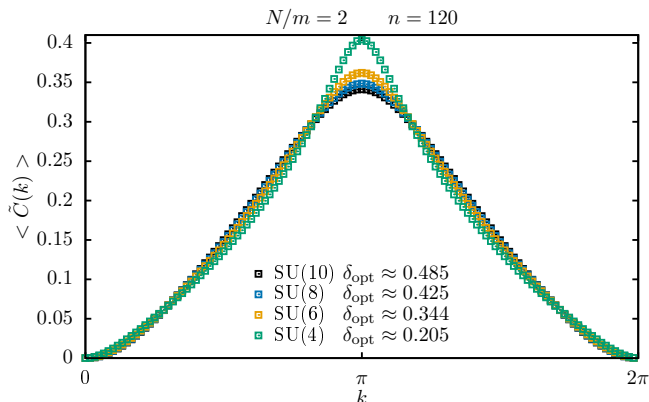


FIG. 4. Structure factor of various $SU(N)$ models with $m = N/2$ calculated with VMC with the optimal variational parameter δ_{opt} .

V. $SU(6)$ WITH $m = 2$

This case is a priori more challenging to study because the relevant operator that is generated in the renormalization group theory appears at higher order than the one-loop approximation. Therefore, the gap can be expected to be significantly smaller than in the previous case. This trend is definitely confirmed by ED performed on clusters with up to 15 sites: the gap decreases quite steeply with the system size (see upper left panel of FIG. 5). It scales smoothly however, and a linear extrapolation points to a gap of the order $\Delta E \simeq 0.2$, much smaller than in the $SU(6)$ case with $m = 3$ ($\Delta E \simeq 4$), but finite. On the largest available cluster, the bond energy has a significant dependence on the bond position, with an alternance of two very negative bonds with a less negative one.

These trends are confirmed and amplified by VMC. Indeed, the trimerized wave function $|\Psi_G^3(\delta)\rangle$ leads to a better energy for all sizes, and the optimal value scales very smoothly to a small but finite value $\delta_{\text{opt}} \approx 0.03$. This value is about an order of magnitude smaller than in the $SU(6)$ case with $m = 3$, but the fact that it does not change with the size beyond 60 sites is a very strong indication that the system trimerizes (by contrast to the marginal case shown in FIG. 9). The trimerization is confirmed by the lower plots. For $n = 15$, the VMC results are again in nearly perfect agreement with ED, and for $n = 60$, the bond energy shows a very clear trimerization.

To test the nature of the long-range correlations is of

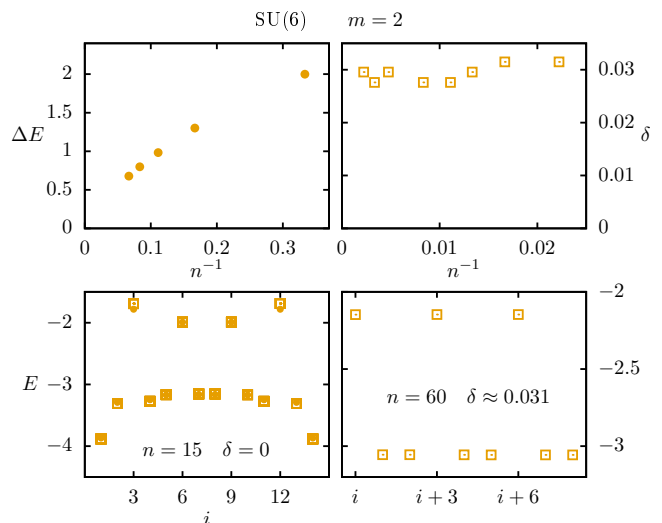


FIG. 5. ED and VMC results for the $SU(6)$ model with $m = 2$. Upper left panel: size dependence of the energy gap. Upper right panel: optimal variational parameter δ for periodic boundary conditions. Lower left panel: energy per bond calculated with ED (circles) and VMC (squares) on 15 sites with open boundary conditions. Note that the optimal variational parameter $\delta = 0$ in that case. Lower right panel: energy per bond calculated with VMC with periodic boundary conditions.

course more challenging than in the previous case since a small gap implies a long correlation length. And indeed, on small to intermediate sizes, the structure factor has a sharp peak at $k = 2\pi/3$ very similar to the $SU(3)$, $m = 1$ case. However, going to very large system sizes (up to

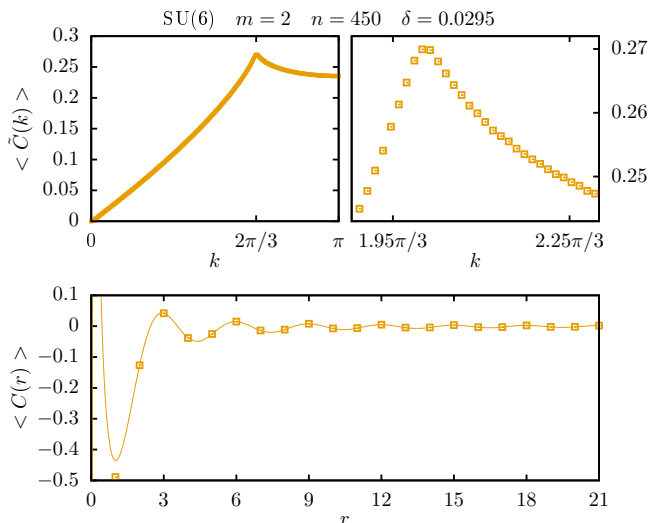


FIG. 6. Upper left panel: Structure factor of the $SU(6)$ model with $m = 2$ calculated with VMC using a trimerized wave function with the optimal variational parameter. Upper right panel: zoom on the region near $k = 2\pi/3$. It clearly shows that the structure factor is smooth. Lower panel: real-space diagonal correlations for 60 sites.

$n = 450$ sites), it is clear that the concavity changes sign upon approaching $k = 2\pi/3$ (see upper right panel of FIG. 6), consistent with a smooth peak, hence with exponentially decaying correlation functions (see also lower panel of FIG. 6).

In that case, in view of the small magnitude of the gap, hence of the very large value of the correlation length, it would be difficult to conclude that the system is definitely trimerized on the basis of ED only. In that respect, the VMC results are very useful. On small clusters, the Gutzwiller projected wave function with trimerization is nearly exact, and VMC simulations on very large systems strongly support the presence of a trimerization and of exponentially decaying correlations⁴⁸.

VI. MARGINAL CASES: SU(8) WITH $m = 2$ AND SU(9) WITH $m = 3$

These two systems are the only ones which possess operators with scaling dimension $\chi = 2$. They are therefore the only cases where it is impossible to predict whether the system is algebraic or gapped on the basis of Affleck's analysis. As far as numerics is concerned, these cases can again be expected to require large system sizes to conclude.

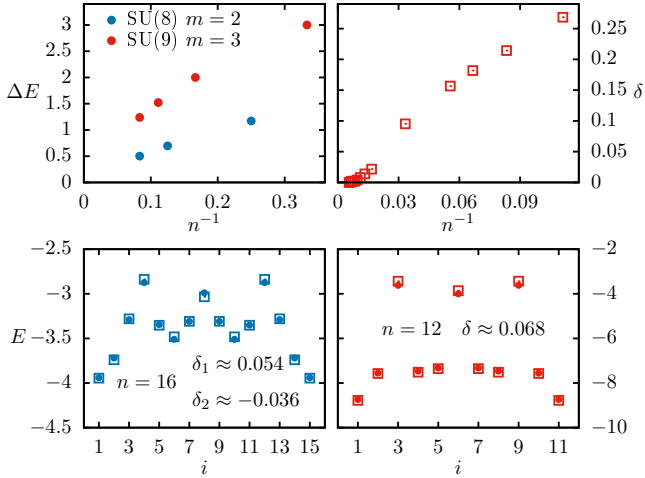


FIG. 7. ED and VMC results for the marginal cases SU(8) with $m = 2$ and SU(9) with $m = 3$. Upper left panel: size dependence of the energy gap for both cases. Upper right panel: optimal variational parameter δ for the SU(9) case with periodic boundary conditions. The results for SU(8) are not shown because they identically vanish for periodic boundary conditions. Lower left panel: energy per bond for SU(8) calculated with ED (circles) and VMC (squares) for open boundary conditions. Note that the optimal variational parameters δ_{opt} are different from zero with open boundary conditions. Lower right panel: energy per bond for SU(9) calculated with ED (circles) and VMC (squares) for open boundary conditions.

The ED results are quite similar to the previous case. The scaling of the gap is less conclusive because the last

three points build a curve that is still concave and not linear like in the previous case (see the upper right panel of FIG. 7). So one can only conclude that if there is a gap, it is very small, especially for SU(8) with $m = 2$. The bond energies build a pattern which is consistent with a weak tetramerization for SU(8) with $m = 2$, and with a significant trimerization comparable to the SU(6), $m = 2$ case for SU(9) $m = 3$.

The VMC method turns out to give a rather different picture however. For SU(8) with $m = 2$, two variational wave functions ($|\Psi_G^{\text{Fermi}}\rangle$, $|\Psi_G^4(\delta_1, \delta_2)\rangle$) can be tested. Interestingly, for $n = 16$ with open boundary conditions, $|\Psi_G^{\text{Fermi}}\rangle$ fails to reproduce the bound energies pattern observed with ED but $|\Psi_G^4(0.054, -0.036)\rangle$ is successful (see lower left panel of FIG. 7). This pattern, which could be interpreted as a weak tetramerization, is in fact probably just a consequence of the four-fold periodicity of algebraic correlations in the presence of open boundary conditions. Indeed, it turns out that, for any system size with periodic boundary conditions, the minimization of the energy using $|\Psi_G^4(\delta_1, \delta_2)\rangle$ failed to find a solution for any $|\delta_{1,2}| > 0.002$. Therefore $|\Psi_G^{\text{Fermi}}\rangle$ is believed to be the best variational wavefunction. The conclusion is that there is no tetramerization, and that the correlations must be algebraic. This is also supported by the structure factor, which seems to have a singularity at $k = \pi/2$ (see FIG. 8).

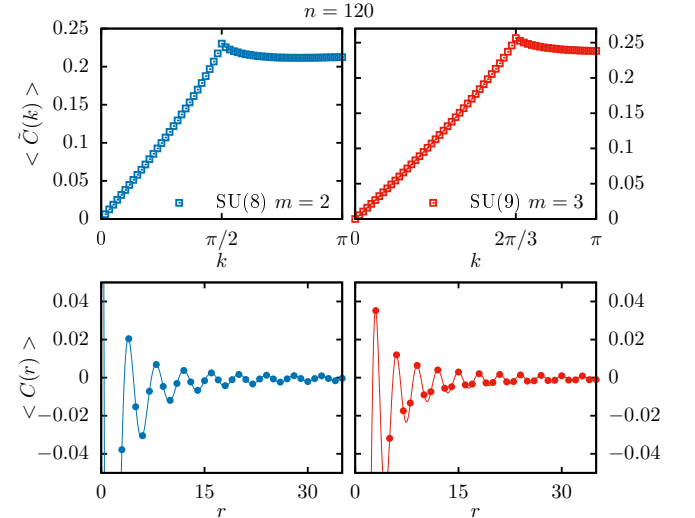


FIG. 8. Upper panels: Structure factor of the SU(8) model with $m = 2$ (left) and of the SU(9) model with $m = 3$ (right) calculated with VMC with periodic boundary conditions. Lower panels: real space correlations. The four plots represents results obtained with $|\Psi_G^{\text{Fermi}}\rangle$.

Let us now turn to SU(9) with $m = 3$. This system could in principle be trimerized, and therefore $|\Psi_G^{\text{Fermi}}\rangle$ and $|\Psi_G^3(\delta)\rangle$ have been compared. For small clusters, there is a large optimal value of δ , actually much larger than for SU(6) with $m = 2$, and the bond energies are typical of a strongly trimerized system, in agreement with

ED. However, δ_{opt} decreases very fast with n until it vanishes for $n \gtrsim 100$ whereas, for SU(6) with $m = 2$, δ_{opt} levels off at a finite value beyond $n = 60$ (see FIG. 9). We interpret this behavior as indicating the presence of a cross-over: on small length scales, the system is effectively trimerized, but this is only a short-range effect, and the system is in fact gapless with, at long-length scale, algebraic correlations.

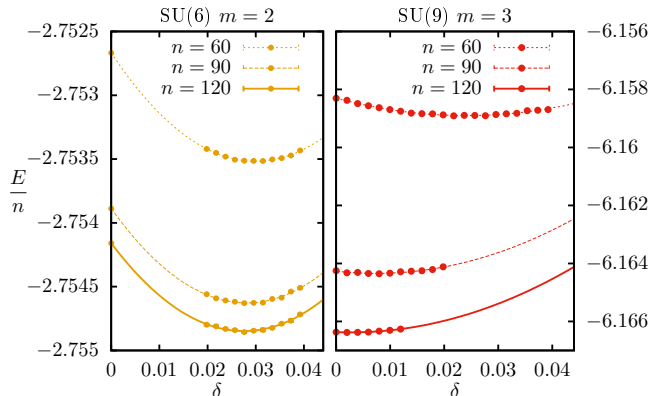


FIG. 9. Energy per site as a function of the variational parameter δ for the SU(6) with $m = 2$ (left) and SU(9) with $m = 3$ (right).

One can again calculate the structure factor using the best variational wave function (in both cases $|\Psi_G^{\text{Fermi}}\rangle$ for big enough systems) to check if a discontinuity exists. The results displayed in the upper plots of FIG. 8 clearly show a discontinuity at $k = \pi/2$ for the SU(8) and at $k = 2\pi/3$ for SU(9). These discontinuities indicate an algebraic decay of the long-range correlations. The lower plot shows that even if these systems are gapless, there is a maxima of the correlation every N/m sites.

VII. EXAMPLE WITH IRRELEVANT OPERATOR: SU(10) WITH $m = 2$

For completeness, we have also looked at a case where there is an irrelevant operator of scaling dimension larger than 2, namely SU(10) with $m = 2$. As expected, the best variational wave function is $|\Psi_G^{\text{Fermi}}\rangle$ for all sizes, and the structure factor exhibits discontinuities at $k = 2\pi/5$, consistent with a gapless spectrum and algebraic correlations.

VIII. CRITICAL EXPONENTS

Motivated by the remarkably accurate results obtained in previous works for the case the fundamental representation^{15,32}, we have tried to use the VMC results to determine the critical exponent that controls the decay of the correlation function at long distance, Eq.7. For the particular case of gapless systems, conformal field theory

predicts an algebraic decay of the long-range correlations function according to:

$$C(r) = \frac{c_0}{r^2} + \frac{c_k \cos(2\pi r m/N)}{r^\eta}$$

where $\eta = 2 - 2/N$ is the critical exponent.

For systems with periodic boundary conditions, one can define two distances between two points, which naturally leads to the following fitting function⁸:

$$c_0(r^{-\nu} + (n-r)^{-\nu}) + c_k \cos(2\pi r m/N) (r^{-\eta} + (n-r)^{-\eta})$$

with four free parameters: c_0 , ν and c_k , η , the amplitudes and critical exponents of the components at $k = 0$ and $k = 2\pi m/N$ respectively.

There is a large degree of freedom in the choice of the fitting range. One could in principle select any arbitrary range of sites $[x_i, x_f]$, $0 \leq x_i < x_f \leq n-1$. The problem is that each range will give different critical exponents. In order to obtain some meaningful results the following method has been chosen. Using the periodicity of the systems, only the ranges with $x_i = a$ and $x_f = n-a-1$, $1 \leq a \leq n/2$, have been considered. For each value of a , the coefficient of determination of the fit has been computed and if its value is higher than 0.999 then the range $[a, n-a-1]$ is selected to perform the extrapolation of the critical exponents. If the value is too low, the fit is considered to be bad and the range with $a \leftarrow a+1$ is tested. If no good range can be found with this criterion, the condition over the coefficient of determination is relaxed to be higher than 0.995 and the first fit with a residual sum of squares divided by n that is smaller than 10^{-7} is selected.

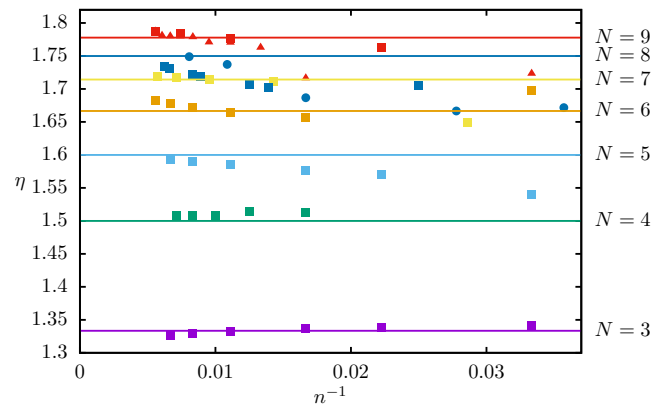


FIG. 10. Critical exponents η of the gapless systems as a function of the system size. The squares, circles and triangles correspond respectively to $m = 1, 2$, and 3 particles per site. All values given here have been calculated with $|\Psi_G^{\text{Fermi}}\rangle$.

The critical exponents η obtained in this way are shown in FIG. 10. The theoretical values of the critical exponents $\eta = 2 - 2/N$ are shown as straight lines. In all cases, the extracted exponents agree quite well with the theoretical predictions when n is large enough. In particular, for a given N , the exponent η does not depend on

m , as predicted by non-abelian bosonization. The critical exponents ν has also been extracted but, as already observed⁸, a precise estimate is difficult to get. Nevertheless, for $N = 3, 4$, $\nu \in [1.8, 2.25]$ and for $N \geq 5$, $\nu \in [1.95, 2.05]$ for the largest systems.

IX. CONCLUSIONS

Using variational Monte Carlo based on Gutzwiller projected wave functions, we have explored the properties of $SU(N)$ Heisenberg chains with various totally antisymmetric irreps at each site. In the case of the fundamental representation, which is completely understood thanks to Bethe ansatz and to QMC simulations, these wave functions are remarkably accurate both regarding the energy and the long-range correlations. In the case of higher antisymmetric irreps, where field theory arguments are in most cases able to predict that the system should be gapless or gapped, allowing for a symmetry breaking term in the tight binding Hamiltonian used to define the unprojected wave function leads to results in perfect agreement with these predictions, and the ground state is found to be spontaneously dimerized or trimer-

ized. Finally, in the two cases where the operator that could open a gap is marginal, $SU(8)$ with $m = 2$ and $SU(9)$ with $m = 3$, this variational approach predicts that there is no spontaneous symmetry breaking, and that correlations decay algebraically. These results suggest that the operators are marginally irrelevant in both cases. It would be interesting to test these predictions either analytically by pushing the renormalization group calculations to higher order, or numerically with alternative approaches such as DMRG or QMC.

In any case, these results prove that Gutzwiller projected fermionic wave functions do a remarkably good job at capturing quantum fluctuations in one-dimensional $SU(N)$ Heisenberg models with totally antisymmetric irreps. Considering the encouraging results obtained in 2D for the $SU(N)$ Heisenberg model with the fundamental irrep at each site on several lattices, one can legitimately hope these wave functions to be also good for the $SU(N)$ Heisenberg model with totally antisymmetric irreps at each site in 2D. Work is in progress along these lines.

We acknowledge useful discussions with S. Capponi, M. Lajko, P. Lecheminant, L. Messio, and K. Penc. This work has been supported by the Swiss National Science Foundation.

-
- ¹ C. Wu, J.-p. Hu, and S.-c. Zhang, *Phys. Rev. Lett.* **91**, 186402 (2003).
 - ² A. V. Gorshkov, M. Hermele, V. Gurarie, C. Xu, P. S. Julianne, J. Ye, P. Zoller, E. Demler, M. D. Lukin, and A. M. Rey, *Nat Phys* **6**, 289 (2010).
 - ³ R. Assaraf, P. Azaria, M. Caffarel, and P. Lecheminant, *Phys. Rev. B* **60**, 2299 (1999).
 - ⁴ F. Scazza, C. Hofrichter, M. Höfer, P. C. De Groot, I. Bloch, and S. Fölling, *Nature Physics* (2014), 10.1038/nphys3061.
 - ⁵ X. Zhang, M. Bishof, S. L. Bromley, C. V. Kraus, M. S. Safronova, P. Zoller, a. M. Rey, and J. Ye, *Science (New York, N.Y.)*, 1 (2014).
 - ⁶ G. Pagano, M. Mancini, G. Cappellini, P. Lombardi, F. Schäfer, H. Hu, X.-J. Liu, J. Catani, C. Sias, M. Inguscio, and L. Fallani, *Nature Physics* **10**, 198 (2014).
 - ⁷ B. Sutherland, *Physical Review B* **12**, 3795 (1975).
 - ⁸ B. Frischmuth, F. Mila, and M. Troyer, *Physical Review Letters* **82**, 835 (1999).
 - ⁹ L. Messio and F. Mila, *Physical Review Letters* **109**, 205306 (2012).
 - ¹⁰ Y. Q. Li, M. Ma, D. N. Shi, and F. C. Zhang, *Phys. Rev. Lett.* **81**, 3527 (1998).
 - ¹¹ M. van den Bossche, F.-C. Zhang, and F. Mila, *The European Physical Journal B - Condensed Matter and Complex Systems* **17**, 367 (2000).
 - ¹² M. van den Bossche, P. Azaria, P. Lecheminant, and F. Mila, *Phys. Rev. Lett.* **86**, 4124 (2001).
 - ¹³ K. Penc, M. Mambrini, P. Fazekas, and F. Mila, *Phys. Rev. B* **68**, 012408 (2003).
 - ¹⁴ D. P. Arovas, *Phys. Rev. B* **77**, 104404 (2008).
 - ¹⁵ F. Wang and A. Vishwanath, *Physical Review B* **80**, 064413 (2009).
 - ¹⁶ T. A. Tóth, A. M. Läuchli, F. Mila, and K. Penc, *Phys. Rev. Lett.* **105**, 265301 (2010).
 - ¹⁷ H.-H. Hung, Y. Wang, and C. Wu, *Phys. Rev. B* **84**, 054406 (2011).
 - ¹⁸ E. Szirmai and M. Lewenstein, *EPL (Europhysics Letters)* **93**, 66005 (2011).
 - ¹⁹ P. Corboz, A. M. Läuchli, K. Penc, M. Troyer, and F. Mila, *Phys. Rev. Lett.* **107**, 215301 (2011).
 - ²⁰ G. Szirmai, E. Szirmai, A. Zamora, and M. Lewenstein, *Phys. Rev. A* **84**, 011611 (2011).
 - ²¹ P. Corboz, K. Penc, F. Mila, and A. M. Läuchli, *Phys. Rev. B* **86**, 041106 (2012).
 - ²² P. Corboz, M. Lajkó, A. M. Läuchli, K. Penc, and F. Mila, *Phys. Rev. X* **2**, 041013 (2012).
 - ²³ B. Bauer, P. Corboz, A. M. Läuchli, L. Messio, K. Penc, M. Troyer, and F. Mila, *Phys. Rev. B* **85**, 125116 (2012).
 - ²⁴ P. Corboz, M. Lajkó, K. Penc, F. Mila, and A. M. Läuchli, *Phys. Rev. B* **87**, 195113 (2013).
 - ²⁵ D. Wang, Y. Li, Z. Cai, Z. Zhou, Y. Wang, and C. Wu, *Phys. Rev. Lett.* **112**, 156403 (2014).
 - ²⁶ M. Hermele, V. Gurarie, and A. M. Rey, *Phys. Rev. Lett.* **103**, 135301 (2009).
 - ²⁷ M. Hermele and V. Gurarie, *Physical Review B* **84**, 1 (2011).
 - ²⁸ F. F. Assaad, *Phys. Rev. B* **71**, 075103 (2005).
 - ²⁹ Z. Cai, H.-H. Hung, L. Wang, and C. Wu, *Phys. Rev. B* **88**, 125108 (2013).
 - ³⁰ T. C. Lang, Z. Y. Meng, A. Muramatsu, S. Wessel, and F. F. Assaad, *Phys. Rev. Lett.* **111**, 066401 (2013).
 - ³¹ Z. Zhou, Z. Cai, C. Wu, and Y. Wang, *Phys. Rev. B* **90**, 235139 (2014).
 - ³² A. Paramekanti and J. B. Marston, *Journal of Physics: Condensed Matter* **19**, 125215 (2007).

- ³³ N. Andrei and H. Johannesson, [Physics Letters A **104**, 370 \(1984\)](#).
- ³⁴ H. Johannesson, [Nuclear Physics B **270**, 235 \(1986\)](#).
- ³⁵ M. Fuhringer, S. Rachel, R. Thomale, M. Greiter, and P. Schmitteckert, [Annalen der Physik **17**, 922 \(2008\)](#).
- ³⁶ S. Rachel, R. Thomale, M. Fuhringer, P. Schmitteckert, and M. Greiter, [Phys. Rev. B **80**, 180420 \(2009\)](#).
- ³⁷ H. Nonne, P. Lecheminant, S. Capponi, G. Roux, and E. Boulat, [Phys. Rev. B **84**, 125123 \(2011\)](#).
- ³⁸ H. Nonne, M. Moliner, S. Capponi, P. Lecheminant, and K. Totsuka, [EPL \(Europhysics Letters\) **102**, 37008 \(2013\)](#).
- ³⁹ T. Morimoto, H. Ueda, T. Momoi, and A. Furusaki, [Phys. Rev. B **90**, 235111 \(2014\)](#).
- ⁴⁰ K. Duivenvoorden and T. Quella, [Phys. Rev. B **86**, 235142 \(2012\)](#).
- ⁴¹ I. Affleck, [Nuclear Physics B **265**, 409 \(1986\)](#).
- ⁴² I. Affleck, [Nuclear Physics B **305**, 582 \(1988\)](#).
- ⁴³ V. Knizhnik and A. Zamolodchikov, [Nuclear Physics B **247**, 83 \(1984\)](#).
- ⁴⁴ M. Lajko and K. Penc, [Physical Review B **87**, 224428 \(2013\)](#).
- ⁴⁵ P. Nataf and F. Mila, [Phys. Rev. Lett. **113**, 127204 \(2014\)](#).
- ⁴⁶ S. Yunoki and S. Sorella, [Phys. Rev. B **74**, 014408 \(2006\)](#).
- ⁴⁷ I. Affleck, D. Arovas, J. Marston, and D. Rabson, [Nuclear Physics B **366**, 467 \(1991\)](#).
- ⁴⁸ We have been informed by S. Capponi that these conclusions agree with unpublished DMRG results (S. Capponi, private communication).